Journal of Power Sources 241 (2013) 410–414

Contents lists available at SciVerse ScienceDirect

Journal of Power Sources

journal homepage: www.elsevier.com/locate/jpowsour

Short communication

Highly textured $Li(Ni_{0.5}Mn_{0.3}Co_{0.2})O_2$ thin films on stainless steel as cathode for lithium-ion battery

Clement Jacob, Tommy Lynch, Aiping Chen, Jie Jian, Haiyan Wang*

Department of Electrical and Computer Engineering, Texas A&M University, College Station, TX 77843-3128, USA

HIGHLIGHTS

- Epitaxial and highly textured $Li(Ni_xMn_yCo_{1-x-y})O_2$ thin films are grown.
- A one-step, high temperature pulsed laser deposition method is used.
- Film microstructure and its effect on battery performance are presented.
- Initial capacity of 167 mAh g^{-1} and 125 mAh g^{-1} is obtained at 0.1 C and 0.5 C.
- Excellent capacity retention of 89% is obtained at 0.5 C after 100 cycles.

ARTICLE INFO

Article history:
Received 25 February 2013
Received in revised form
25 April 2013
Accepted 26 April 2013
Available online 9 May 2013

Keywords:
$Li(Ni_xMn_yCo_{1-x-y})O_2$
Thin film
Epitaxial
Pulsed laser deposition
Lithium ion battery
High temperature

ABSTRACT

Epitaxial and highly textured $Li(Ni_xMn_yCo_{1-x-y})O_2$ thin film cathodes are deposited by a one-step, high temperature pulsed laser deposition technique. Structural characterization using X-ray diffraction, transmission electron microscopy and selected area electron diffraction (SAED) reveals highly textured film along (003). The best film quality has been achieved at high temperature, with temperature as high as 750 °C. Different substrates and buffer layers have been investigated and $Li(Ni_{0.5}Mn_{0.3}Co_{0.2})O_2$ (NMC) on stainless steel with a thin Au-buffer layer gives the best film quality. The NMC thin film cathodes give a high capacity of 167 mAh g^{-1} and 125 mAh g^{-1} at 0.1 C and 0.5 C, respectively. In addition, the cyclic voltammetry and charge discharge curves obtained after different cycles indicate good electrochemical stability with capacity retention of 89% after 100 cycles at 0.5 C. The electrochemical characteristics are correlated to the microstructure of the film and the effects of texture, grain size and density are discussed.

1. Introduction

Thin film cathode research has been extensively pursued toward the development of solid state battery [1–6]. Thin film cathodes have also been proven to be a useful tool for investigating the properties of the intrinsic material. $LiCoO_2$ is by far the most popular and well researched material amongst transitional metal oxides for lithium ion batteries [7–9]. However it suffers several shortcomings including poor stability, inability to extract all the lithium ions and the high cost and toxicity of cobalt [10,11]. One of the most successful strategies to overcome some of these limitations, is the partial substitution of Co with Ni and Mn to form $Li(Ni_xMn_yCo_{1-x-y})O_2$. Ohzuku and Makimura [12], and Lu and Dahn [13] first reported this in 2001. $Li(Ni_xMn_yCo_{1-x-y})O_2$ has a structure similar to $LiCoO_2$, α-$NaFeO_2$ type structure and $R\bar{3}m$ space group. Ohzuku and co-workers reported a capacity of 150 mAh g^{-1} for $Li(Co_{1/3}Ni_{1/3}Mn_{1/3})O_2$ cell cycled between 2.5 V and 4.2 V. There is a renewed interest in transition metal oxides, especially multi-cation Ni, Mn and Co based oxides with the introduction of high capacity transition metal oxide composite [14–17] and core shell structure [18,19]. Thin film batteries can be very useful in exploring such novel materials both for fundamental research and solid state batteries.

Thin film cathode fabrication has been explored over the last two decades [1,20,21], primarily using Radio Frequency (RF) sputter [1,20,22–27] and pulsed laser deposition (PLD) [27–36]. However, very little work has been done on thin film $Li(Ni_xMn_yCo_{1-x-y})O_2$ cathodes. A detailed examination of the film growth could lead to a better understanding of its crystal structure and offer great opportunity to identify stable and high performance cathode material.

* Corresponding author.
E-mail address: wangh@ece.tamu.edu (H. Wang).

0378-7753/$ – see front matter © 2013 Elsevier B.V. All rights reserved.
http://dx.doi.org/10.1016/j.jpowsour.2013.04.140

Traditionally high quality films and novel material synthesis requires high temperature deposition. However the only reports in literature for $Li(Ni_xMn_yCo_{1-x-y})O_2$ thin film are those with room temperature (RT) deposition followed by post anneal. Also ambiguity remains about the benefits of the high temperature post annealing. Deng and others observed poor cyclability and adhesion for films annealed above 500 °C [26]. Ding and co-workers reported an RT RF sputtering of $Li(Co_{1/3}Ni_{1/3}Mn_{1/3})O_2$ followed by a post anneal step at 700 °C, however their results is not conclusive as the cyclability is also limited by the interfacial stability of the solid electrolyte used in the experiment [24]. Xie et al. reported good initial capacity for films annealed at 600 °C for RF sputtered film, but did not investigate cycling capability of the cathodes [25]. Also post annealing of films in all these cases resulted in either amorphous or randomly oriented polycrystalline films. Low temperature amorphous or polycrystalline films can be useful for flexible batteries specially coupled with solid electrolyte like lithium phosphorous oxynitride (LiPON). However, unlike crystalline metal oxide films, which have good conductivity due to sharing of the metal cations between adjacent unit cells, amorphous films tend to impede electron flow [37]. A PLD with in-situ heating allows for a one step process for fabricating thin film cathodes. Furthermore in addition to cost benefits, it gives the capability to control film microstructure by varying oxygen partial pressure, deposition frequency, temperature and deposition energy. In this work, one step, high temperature deposition of $Li(Ni_{0.5}Mn_{0.3}Co_{0.2})O_2$ (NMC) thin film and its cycling performance is reported. The effects of different substrates and buffer layers on the film crystallography and the electrochemical characteristics of the batteries are investigated.

2. Experimental

NMC thin film cathodes were prepared by PLD using a Lambda Physik KrF excimer laser with a wavelength of 248 nm and energy of 180 mJ–400 mJ. The laser energy of 200 mJ corresponding to a laser energy density of 6 J cm^{-2} was applied to achieve high quality deposition of NMC film. Commercial NMC powder (MTI; average particle size of 10 μm and Brunauer–Emmett–Teller (BET) surface area of 0.2–0.6 m^2 g^{-1}) was used for all experiments. To compensate the possible loss of lithium during target calcination and laser ablation during deposition, 20% excess Li was used for the target. The target was prepared by mixing stoichiometric powder with 20% Li_2CO_3 powder (99.99% Alfa Asear). The mixture was first heated at 350 °C, pressed into a pellet and sintered at 900 °C for 12 h in air. Different substrates were used including Silicon (111), stainless steel (SS) and *c*-cut sapphire (0001). In addition buffer layer coating of gold (Au) and titanium nitride (TiN) were also used. These will be referred to as Au–SS and TiN–SS respectively. A standard DC sputter system was used for the Au buffer, while TiN was deposited using PLD, at room temperature. The substrate temperature was varied from room temperature to 750 °C during PLD deposition to explore the optimum deposition temperature. Conventional thick film cathodes were also prepared using doctor blade method. A slurry containing 84% NMC, 8% Carbon C45 (Timcal) and 8% polyvinylidene fluoride, (Kureha KF100 binder) and *N*-methyl-2-pyrrolidinone (NMP) solvent was mixed using ball milling. A doctor blade applicator was then used to coat the slurry on an aluminum current collector followed by drying at 90 °C for 12 h in air. The film was then pressed and cut into circular cathode discs. The cathode had an average loading of 8 mg cm^{-2}.

The structure and crystallinity of the PLD and doctor blade films were investigated using a Bruker D8 powder X-ray diffractometer. Transmission electron microscopy (TEM) was done using a FEI Tecnai G2 F20 TEM. Coin cells were assembled with lithium metal anode and EC:DEC:1 M $LiPF_6$ (BASF) electrolyte in an argon glove box with well controlled oxygen and moisture levels ($O_2 < 0.1$ ppm and $H_2O < 0.1$ ppm). Galvanostatic charge–discharge cycling tests were carried out between 3 V and 4.2 V at a constant current density of 22 μA cm^{-2} corresponding to 0.5 C, and cyclic voltammetry curves were obtained using a voltage ramp rate of 100 μV s^{-1} both using the Arbin BTS2000 battery testing system. Impedance spectra were measured on a Gamry Series G 300 setup.

3. Results and discussion

The θ–2θ X-ray diffraction scans of the films deposited on different substrates are given in Fig. 1. Bare stainless steel and silicon give weak (003) peaks. The Au–SS sample shows strong NMC (003) peak and a strong Au (111) peak. The single crystal *c*-cut sapphire displays strong (003), (006) and (009) NMC peaks. The film quality is strongly influenced by the laser fluence and substrate temperature. However since the SS and Si ones did not show a strong (003) peak it is obvious that there is a substrate dependence of the film quality. It is possible that the Au-buffer layer helps due to its inert nature or acts like a diffusion barrier between stainless steel and the NMC film. Also the lattice match between Au and NMC can be a contributing factor. Yet another possibility is the surface quality of the substrate. To further investigate the role of buffer layer as diffusion barrier, TiN coating, a known diffusion barrier was tested. However the TiN buffer sample did not show significant improvement in film crystallinity over the others. This suggests that diffusion barrier may not be the dominating factor. Alternatives to gold buffer are attractive due to obvious cost benefits. Further work on TiN and other alternate buffers is currently underway. Si (111) (3.136 Å) and NMC (2.867 Å) have a much larger mismatch compared to the 0.62% mismatch between Au and NMC. This directly correlates to the observed film quality. It was initially expected that high temperature should enable textured film irrespective of the substrate. It is possible that the roughness of the surface of the bare substrate also adversely affected the film quality. The textured nature of the Au-coated substrate likely offsets this as well. Fig. 2 shows films deposited on Au–SS substrates at different

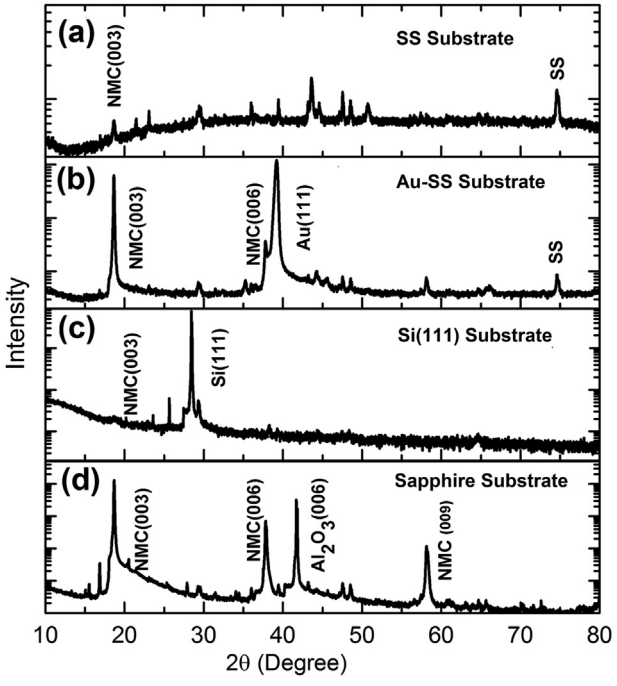

Fig. 1. XRD patterns of PLD deposited thin films of $Li(Ni_{0.5}Mn_{0.3}Co_{0.2})O_2$ on (a) Stainless steel; (b) Au-coated stainless steel; (c) Silicon (111); and (d) *c*-cut sapphire.

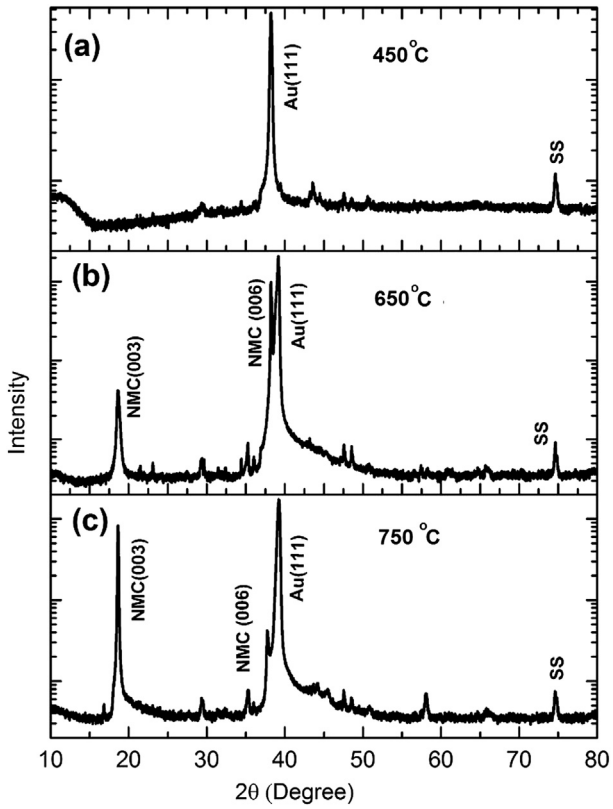

Fig. 2. XRD patterns of NMC films deposited on Au–SS substrate at (a) 450 °C; (b) 650 °C; and (c) 750 °C.

temperatures. At deposition temperatures below 500 °C no significant film peaks were observed. The (003) peaks starts to show up as the deposition temperature increases to 650 °C and is very strong for films deposited at 750 °C. This is expected as high density, epitaxial film growth can be achieved at high temperatures. In case of $LiCoO_2$, temperatures above 700 °C have been reported to cause impurity phases. However no such impurity phase is observed for NMC in this study. This can be attributed to the stability of the structure which prevents the formation of Co_3O_4 or any other secondary phases. Another phenomenon observed is the reduction of the (006) peak intensity with increase in temperature. A strong (003) peak and weak (006) peak is very typical for PLD thin films of this class of material [31]. An inexpensive conducting substrate is preferred for actual electrochemical tests while high quality single crystal substrate is desirable for initial studies and film analysis. To compare the quality of the film on the Au–SS and sapphire substrate, the full width half maxima (FWHM) of the substrate peak and (003) peaks on both substrates is compared. The FWHM of the NMC (003) peak on the Au–SS substrate and sapphire is 0.123° and 0.096° respectively. This clearly indicates that high quality film has been achieved on the Au–SS substrate.

The TEM images and the corresponding selected area electron diffraction (SAED) pattern of the film on sapphire substrate from [0$\bar{1}$10] zone axis are shown in Fig. 3. The film has grown epitaxially on sapphire (0001) substrate. The film thickness is approximately 450 nm. The spacing between successive planes corresponds to approximately 4.72 Å which is in agreement with XRD results. The *d*-spacing of (006) estimated from the SAED is 2.39 Å and matches with the theoretical models. The SAED analysis gives the lattice parameters of $a = 2.83 \pm 0.01$ Å and $c = 14.06 \pm 0.01$ Å, which is slightly lower than bulk value reported in literature [38]. In addition the distinguished diffraction dots observed for NMC film

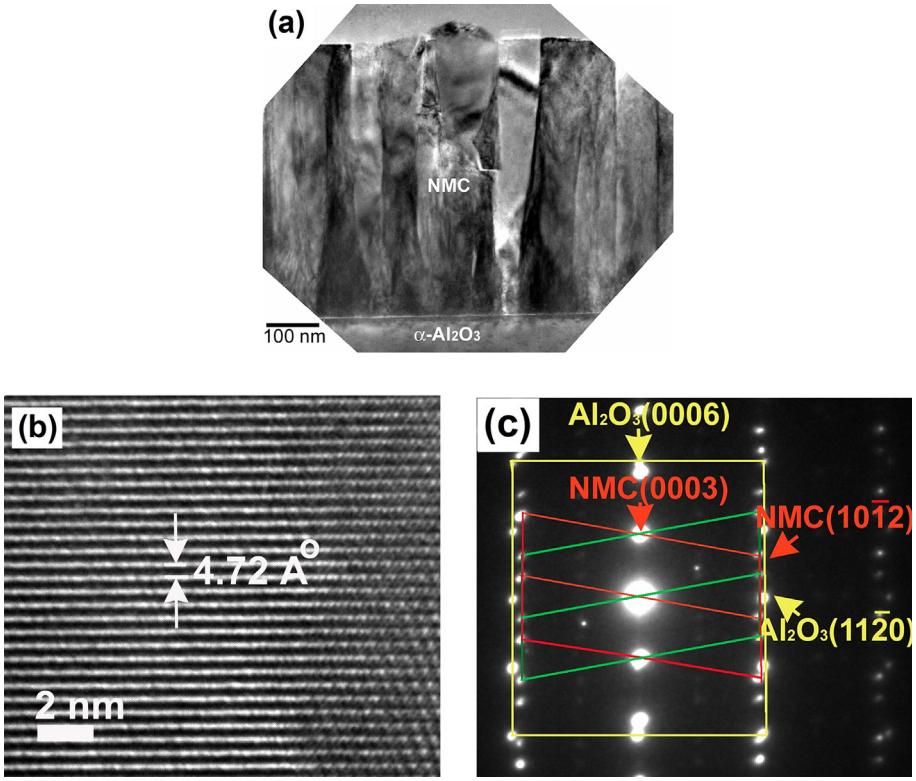

Fig. 3. TEM images of NMC thin film on *c*-cut sapphire substrate: (a) Low magnification image showing columnar NMC film; (b) High resolution TEM image of NMC film; (c) Diffraction pattern of NMC film with sapphire substrate.

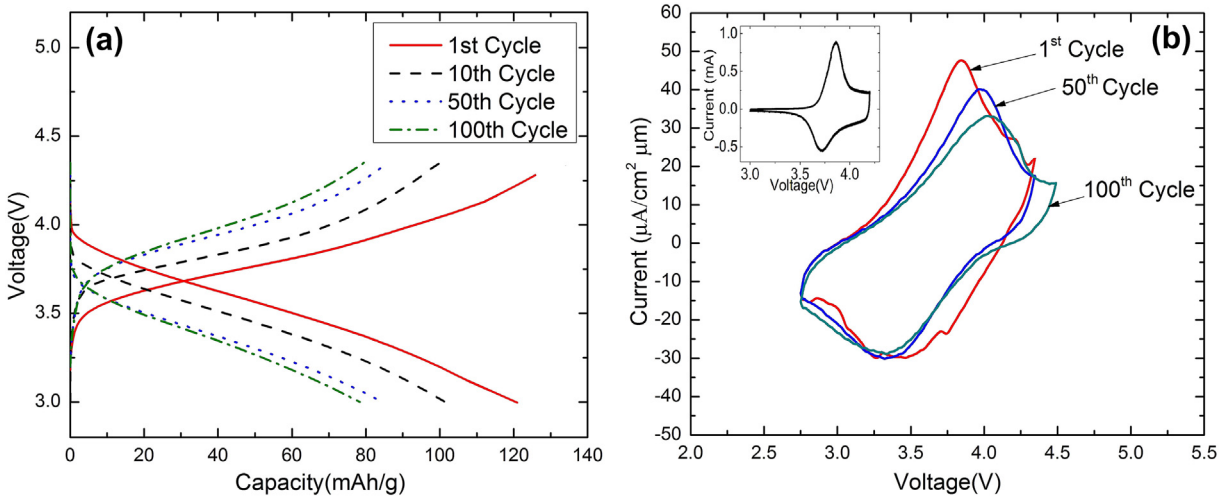

Fig. 4. (a) Charge–discharge curve of battery with NMC thin film cathode on Au–SS substrate after different numbers of cycles; (b) Cyclic voltammetry curve for thin film cathode on Au–SS substrate after different numbers of cycles; inset shows CV curve for battery with thick film NMC cathode.

indicate high quality epitaxial growth of NMC film. The epitaxial relationship between the film and the substrates are determined to be (0002) Al_2O_3// (0003) NMC and [0$\bar{1}$10] Al_2O_3// [$\bar{1}$2$\bar{1}$0] NMC.

The charge–discharge curves after different numbers of cycles for the NMC film on Au–SS substrates are shown in Fig. 4(a). After the initial cycling the relative change in capacity in subsequent cycles reduces. This is probably due to the progressive stabilization of the cathode and decrease in side reactions. While EC:DEC 1 M LiPF6 is stable up to 4.3 V, there could still be partial decomposition of electrolyte or reaction at the cathode surface at lower voltages. This could be partially mitigated by a thin coating of solid electrolyte like LiPON, which is a much more stable electrolyte. A sharper discharge curve is seen in Fig. 4(a), than observed for conventional doctor blade films prepared using the same active material. This can be possibly attributed to the polarization at the cathode. Bouwman and co-workers attributed the polarization and faster discharge rate to the (003) orientation of the film, typical of PLD films [27]. The cyclic voltammetry curve for the cells at different cycling stages is given in Fig. 4(b). It clearly shows a broad anodic peak at 3.85 V and a broad cathodic peak at 3.5 V corresponding to Ni^{2+}/Ni^{4+} redox process, after the 1st cycle. The CV curve for a thick film battery, prepared using the conventional doctor blade method is shown in the inset. The anodic and cathodic peaks at 3.85 V and 3.7 V are sharper compared to the thin film samples. The shift seen in the cathodic peak is believed to be a result of the fast scan rate. Limited by our measurement capability, the larger scan rates could result in the electrochemical reactions occurring at the surface rather than in the bulk of the film. Another possible contributing factor to the shift as well as the peak broadening is the polarization due to the large grain size and a lack of conductive additives [39]. After the 50th and 100th cycle the anodic peak shifts to 3.95 V and 4 V respectively, while the cathodic peak position does not show a significant shift. Usually, an increase in peak separation is associated with a decrease in reversibility. However it seems that the increased peak separation occurs due to a combination of the same factors that also resulted in peak shifts discussed earlier. In addition a reduction in the current amplitude of the anodic peak can be seen. This is most likely due to increase in surface resistance of the cathode with increased cycling. Also, consistent to the data seen in individual cycles in Fig. 4(a), the

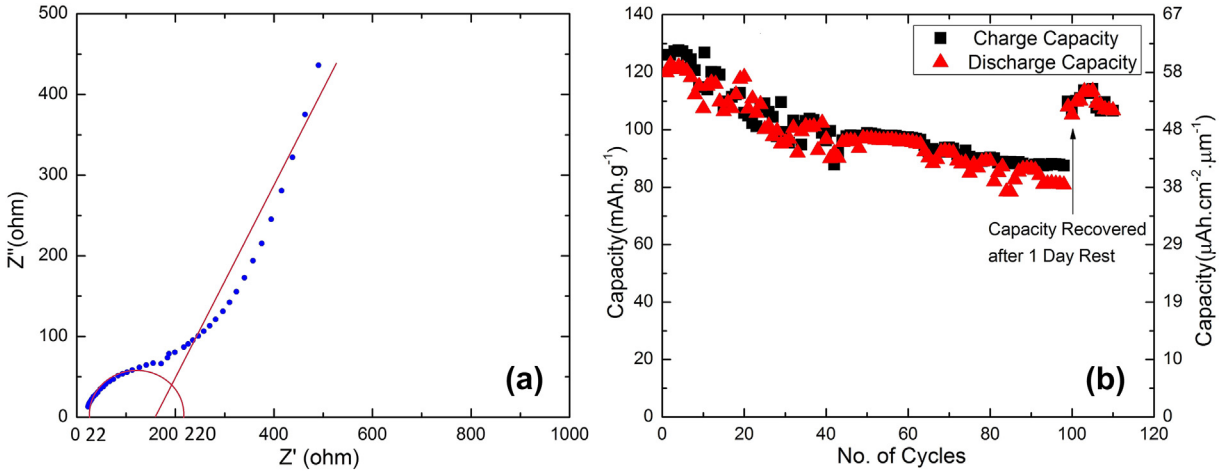

Fig. 5. (a) Electrochemical impedance spectroscopy of NMC thin film on Au–SS substrates; (b) Charge–discharge capacity of NMC thin film cathode on Au–SS substrate as a function of cycle number.

difference between the peak amplitudes reduces progressively with cycling, indicating a good structural stability during the intercalation and de-intercalation of Li ions. Fig. 5(a) gives a typical electrochemical impedance spectroscopy (EIS) measurement of the cell. The solution resistance and ohmic contact resistance is around 22 Ω while the charge transfer resistance of 275 Ω. The low ohmic resistance is probably due to good adhesion. Kim and coworkers reported that (003) oriented film in $LiCoO_2$ exhibit the least volume expansion during cycling at high voltages as compared to randomly oriented powder samples [40]. NMC has a similar crystal structure. If the volume expansion during cycling is limited the corresponding increase in interfacial stress between the current collector and cathode film during cycling will be reduced. Since the film substrate adhesion during cycling is excellent, the cycling performance of the battery is improved. The diffusion or Warburg resistance dominates the impedance in the mid and low frequency region. Thin films deposited on Au–SS substrate have a capacity of 125 mAh g^{-1} at 0.5 C. This is higher than the values reported in low temperature annealed films at similar charge discharge rate [26]. Furthermore, the high density of the film improves internal adhesion of the film and consequently improves the cycle life of the battery. The charge–discharge capacity of NMC thin film cathodes using Au–SS substrate is shown in Fig. 5(b). The capacity is lower than that reported for bulk batteries. The conductive additives in bulk batteries improve electron transfer, while the film porosity allows better contact with the electrolyte, facilitating improved Li ion transfer. However, thin film cathode do not have inactive mass like carbon and binder and more importantly allows study of material properties independent of such external factors. The cathodes demonstrate good reversibility with 72% capacity retention at 0.5 C after continuous cycling for 100 cycles. Also after resting for a day the cell recovered its capacity significantly. This indicates to a partial reversible capacity loss, probably due to an increase in the polarization of the cathode. The batteries retained 89% of the initial capacity at 0.5 C rate.

4. Conclusion

NMC films were prepared using a one-step high temperature pulsed laser deposition without a separate post-anneal step. The film quality displays strong substrate dependence and Au-buffered stainless steel substrate is found to be an ideal substrate. The textured nature of the Au-buffer layer and good lattice match between Au and NMC contribute to the high quality NMC film growth. TEM and XRD confirm the highly textured and epitaxial quality of the film. The cyclic voltammetry results show peak shifts due to polarization but this does not adversely affect the cycling capacity of the film. The thin film NMC cathode demonstrated an initial capacity of 125 mAh g^{-1} at 0.5 C and retained 89% capacity after 100 cycles. The high cyclability is attributed to the good adhesion between the film and substrate as well as the internal adhesion of the high density film. This work demonstrates the high quality film directly grown by PLD at high temperature without the need for additional post-annealing. This method can be applied to the investigation of more complex cathode structure and composite films for solid state batteries.

Acknowledgments

The TEM work is partially funded by the U.S. National Science Foundation (NSF 0846504). The authors acknowledge the generous material support by BASF (Dr. Megan O'Meara and Dr. Klaus Kuehling), Timcal Graphite and Carbon, (Gustavo Michels) and Kureha America, LLC. (Danuta Zielinska and Yoshikazu Amano).

References

[1] J.B. Bates, N.J. Dudney, D.C. Lubben, G.R. Gruzalski, B.S. Kwak, Xiaohua Yu, R.A. Zuhr, J. Power Sources 54 (1995) 58.
[2] N.J. Dudney, Mater. Sci. Eng. B 116 (2005) 245.
[3] D. Golodnitsky, M. Nathan, V. Yufit, E. Strauss, K. Freedman, L. Burstein, A. Gladkich, E. Peled, Solid State Ionics 177 (2006) 2811.
[4] A. Patil, V. Patil, D.W. Shin, J.-W. Choi, D.-S. Paik, S.-J. Yoon, Mater. Res. Bull. 43 (2008) 1913.
[5] D. Liu, G. Cao, Energy Environ. Sci. 3 (2010) 1218.
[6] S.J. Dillon, K. Sun, Curr. Opin. Solid State Mater. Sci. 16 (2012) 153.
[7] K. Ozawa, Solid State Ionics 69 (1994) 212.
[8] Y.S. Jung, A.S. Cavanagh, A.C. Dillon, M.D. Groner, S.M. George, S.-H. Leea, J. Electrochem. Soc. 157 (1) (2010) A75.
[9] R. Ruffo, C. Wessell, R.A. Huggins, Y. Cui, Electrochem. Commun. 11 (2009) 247.
[10] M.S. Whittingham, Chem. Rev. 104 (2004) 4271.
[11] J.M. Tarascon, M. Armand, Nature 414 (2001) 359.
[12] T. Ohzuku, Y. Makimura, Chem. Lett. 30 (2001) 642.
[13] Z. Lu, D.D. MacNeil, J.R. Dahn, Electrochem. Solid-State Lett. 4 (12) (2001) A200.
[14] M.M. Thackeray, S.-Ho. Kang, C.S. Johnson, J.T. Vaughey, R. Benedek, S.A. Hackney, J. Mater. Chem. 17 (2007) 3112.
[15] J. Gao, J. Kim, A. Manthiram, Electrochem. Commun. 11 (2009) 84.
[16] F. Amalraj, D. Kovacheva, M. Talianker, L. Zeiri, J. Grinblat, N. Leifer, G. Goobes, B. Markovsky, D. Aurbach, J. Electrochem. Soc. 157 (2010) A1121.
[17] H. Yu, H. Kim, Y. Wang, P. He, D. Asakura, Y. Nakamura, H. Zhou, Phys. Chem. Chem. Phys. 14 (2012) 6584.
[18] K.-S. Leea, S.-T. Myungb, Y.-K. Suna, J. Power Sources 195 (2010) 6043.
[19] G.M. Koenig Jr., I. Belharouak, H. Deng, Y.-K. Sun, K. Amine, Chem. Mater. 23 (2011) 1954.
[20] J.B. Bates, N.J. Dudney, B. Neudecker, A. Ueda, C.D. Evans, Solid State Ionics 135 (2000) 33.
[21] C.-L. Liao, K.-Z. Fung, J. Power Sources 128 (2004) 263.
[22] J. Hong, C. Wang, N.J. Dudney, M.J. Lance, J. Electrochem. Soc. 154 (8) (2007) A805.
[23] Q. Shi, R. Hu, L. Ouyang, M. Zeng, M. Zhu, Electrochem. Commun. 11 (2009) 2169.
[24] J.-J. Ding, Q. Sun, Z.-Wen Fu, Electrochem. Solid-State Lett. 13 (8) (2010) A105.
[25] J. Xie, N. Imanishi, T. Zhang, A. Hirano, Y. Takeda, O. Yamamoto, J. Power Sources 195 (2010) 5780.
[26] J. Deng, L. Xi, L. Wang, Z. Wang, C.Y. Chung, X. Han, H. Zhou, J. Power Sources 217 (2012) 491.
[27] P.J. Bouwman, B.A. Boukamp, H.J.M. Bouwmeester, P.H.L. Notten, Solid State Ionics 152–153 (2002) 181.
[28] F. Sauvage, E. Baudrin, M. Morcrette, J.M. Tarascon, Electrochem. Solid-State Lett. 7 (1) (2004) A15.
[29] I. Yamada, T. Abe, Y. Iriyama, Z. Ogumi, Electrochem. Commun. 5 (2003) 502.
[30] N. Kuwata, R. Kumar, K. Toribami, T. a. Suzuki, T. Hattori, J. Kawamura, Solid State Ionics 177 (2006) 2827.
[31] H. Xia, L. Lua, Electrochim. Acta 52 (2007) 7014.
[32] M.C. Rao, J. Crystal Growth 312 (2010) 2799.
[33] N. Imanishi, K. Shizuka, T. Matsumura, A. Hirano, Y. Takeda, R. Kannob, J. Power Sources 174 (2007) 751.
[34] T. Matsumura, N. Imanishi, A. Hirano, N. Sonoyama, Y. Takeda, Solid State Ionics 179 (2008) 2011.
[35] T. Dumont, T. Lippert, M. Dobeli, H. Grimmer, J. Ufheil, P. Novak, A. Wursig, U. Vogt, A. Wokaun, Appl. Surf. Sci. 252 (2006) 4902.
[36] H. Xia, L. Lua, Y. Shirley Meng, Appl. Phys. Lett. 92 1 (2008) 011912.
[37] J.F. Whitacre, W.C. West, E. Brandon, B.V. Ratnakumar, J. Electrochem. Soc. 148 (10) (2001) A1078.
[38] K.M. Shaju, G.V.S. Rao, B.V.R. Chowdari, Electrochim. Acta 48 (2002) 145.
[39] K.C. Jiang, S. Xin, J.S. Lee, J. Kim, X.L. Xiao, Y.G. Guo, Phys. Chem. Chem. Phys. 14 (2012) 2934.
[40] Y.J. Kim, E.-K. Lee, H. Kim, J. Cho, Y.W. Cho, B. Park, S. Mo Oh, J.K. Yoon, J. Electrochem. Soc. 151 (2004) A1063.